# Spectral and thermodynamic properties of the Sachdev-Ye-Kitaev model

Antonio M. García-García[1,*] and Jacobus J. M. Verbaarschot[2,†]

[1]*TCM Group, Cavendish Laboratory, University of Cambridge,
JJ Thomson Avenue, Cambridge CB3 0HE, United Kingdom*
[2]*Department of Physics and Astronomy, Stony Brook University, Stony Brook, New York 11794, USA*

We study spectral and thermodynamic properties of the Sachdev-Ye-Kitaev model, a variant of the $k$-body embedded random ensembles studied for several decades in the context of nuclear physics and quantum chaos. We show analytically that the fourth- and sixth-order energy cumulants vanish in the limit of a large number of particles $N \to \infty$, which is consistent with a Gaussian spectral density. However, for finite $N$, the tail of the average spectral density is well approximated by a semicircle law. The specific heat coefficient, determined numerically from the low-temperature behavior of the partition function, is consistent with the value obtained by previous analytical calculations. For energy scales of the order of the mean level spacing we show that level statistics are well described by random matrix theory. Due to the underlying Clifford algebra of the model, the universality class of the spectral correlations depends on $N$. For larger energy separations we identify an energy scale that grows with $N$, reminiscent of the Thouless energy in mesoscopic physics, where deviations from random matrix theory are observed. Our results are a further confirmation that the Sachdev-Ye-Kitaev model is quantum chaotic for all time scales. According to recent claims in the literature, this is an expected feature in field theories with a gravity dual.

## I. INTRODUCTION

The insurmountable technical difficulties posed by the theoretical description of the many-body nuclear forces have led to many effective descriptions of nuclei to bypass the microscopic Hamiltonian. A crude assumption is to replace the nuclear Hamiltonian with a random matrix ensemble [1–7] only constrained by global symmetries (the Wigner-Dyson ensembles). Surprisingly good agreement was found between spectral correlations of highly excited nuclei and the analytical predictions of random matrix theory for energy scales of the order of the mean level spacing. Despite its success, this approximation has evident shortcomings. The nuclear shell model suggests that nuclear interactions are well described by a mean field potential plus a residual two-body interaction, while in the random matrix approach higher many-body interactions are equally important. Moreover, it was noticed that the spectral density associated with these nuclear excitations did not follow the semicircle law, the random matrix theory prediction, but it is better approximated by the Bethe formula [8].

In response to these problems, a model of fermionic random $k$-body interactions of infinite range, the so called $k$-body embedded ensembles, was proposed more than forty years ago [9–12] as a more accurate stochastic description of nuclei. Although the interactions are random, the effective Hamiltonian is sparse, and therefore deviations

from the Wigner-Dyson ensembles were expected. Indeed, numerical [10] and later analytical results [13] show that, in line with the experimental data, the spectral density is Gaussian for sufficiently small $k$, instead of following the semicircle law. By contrast, spectral correlations are still close to the random-matrix prediction [14] for sufficiently close eigenvalues. For more information on the model, especially in the context of nuclear physics and quantum chaos, we refer to Refs. [15–19].

Recently, similar models of fermions with $k$-body infinite-range interactions, called Sachdev-Ye-Kitaev models (SYK) [20–32], and originally introduced in the study of spin liquids [33], are being intensively investigated in a completely different context: holographic dualities in string theory [34]. Based on the same pattern of conformal symmetry breaking, it has been speculated [20–24,35,36] that, in the infrared limit, the holographic dual of an anti–de Sitter (AdS) background in two bulk dimensions $AdS_2$ is closely related to one of the variants of the SYK model— namely, a model of $N$ Majorana fermions [20] in zero spatial dimensions with random two-body interactions of infinite range. Green's functions [21,22,27,28], thermodynamic properties [29], such as the low-temperature limit of the entropy, and also out-of-equilibrium features [21] such as the exponential growth of certain out-of-time-ordered correlators are strikingly similar in both models. The latter, related to quantum corrections in the gravity dual [37], is also a signature of quantum chaotic features. More interestingly, it is believed that the SYK model may describe the low-energy limit of a higher-dimensional gauge theory with a string theory dual still to be named. Very recent results

[*]amg73@cam.ac.uk
[†]jacobus.verbaarschot@stonybrook.edu

[38] suggest that disorder is not strictly necessary for a gravity-dual interpretation.

Despite these advances, the description of many aspects of the SYK model dynamics still poses severe technical, both numerical and analytical, challenges. In closely related problems such as quantum chaos and disordered systems, the spectrum and level statistics provide a rather comprehensive description of the quantum dynamics without the need of the more expensive computation of eigenvectors. In the context of the SYK model, spectral correlations have so far been investigated in Ref. [30], where level repulsion was found, typical of a disordered metal, though its strength changes with the number of particles $N$ modulo 8.

Here we aim to fill this gap by carrying out an extensive analysis of the spectral density, thermodynamical properties, and both short-range and long-range spectral correlations of the SYK model, with $N$ Majorana fermions.

Our main results are summarized as follows: we show analytically that in the $N \to \infty$ limit the fourth and sixth cumulants of the spectral density vanish, which strongly suggests that it is Gaussian. However, its tail at finite $N$, that controls the specific heat, is well approximated by the semicircle law. Results from exact diagonalization, for up to $N = 36$ Majorana fermions, are fully consistent with the analytical findings, including results for the entropy and the specific heat. Spectral correlations that test short-range correlations such as the level spacing distribution are in good agreement with the random matrix prediction. We find that, in agreement with Ref. [30], the Bott periodicity of the Clifford algebra that governs the Majorana fermions labels the global symmetries of the model. However, we have observed systematic deviations from the random matrix predictions, for sufficiently well separated eigenvalues, that suggest that the model is not ergodic for short times. The point of departure from the universal results of random matrix theory increases with $N$, which is a strong indication of the existence of a Thouless energy [39–41] for the system.

This paper is organized as follows: in the next section we introduce the model and discuss its spectral density. The thermodynamical properties of the model are evaluated in Sec. III. Spectral correlations are computed in Sec. IV. We finish with concluding remarks and some ideas for future research in Sec. V. Some technical details involving the calculation of the cumulants and the symmetry properties of the gamma matrices are worked out in two appendixes.

## II. THE SPECTRAL DENSITY

Kitaev recently introduced [20] a model of interacting fermions aimed to explore its potential as a gravity dual. The Hamiltonian is given by

$$H = \frac{1}{4!} \sum_{i,j,k,l=1}^{N} J_{ijkl}\, \chi_i \chi_j \chi_k \chi_l, \tag{1}$$

where $\chi_i$ are Majorana fermions that verify

$$\{\chi_i, \chi_j\} = \delta_{ij}. \tag{2}$$

The fermions are coupled by Gaussian distributed random variables $J_{ijkl}$ with probability distribution

$$P(J_{ijkl}) = \sqrt{\frac{N^3}{12\pi J^2}} \exp\left(-\frac{N^3 J_{ijkl}^2}{12 J^2}\right). \tag{3}$$

We note that Eq. (2) is the defining relation of a Euclidean $N$-dimensional Clifford algebra. Many interesting features of the model are a direct consequence of Clifford algebra properties. For instance, the Bott periodicity of the Clifford algebra suggests that the global symmetries of the Majorana fermions, that to some extent control the spectral properties of the model, are sensitive to the arithmetic nature of $N$. We shall see that this is indeed the case when we study level statistics later in the paper. It will also be helpful for our first objective: to derive analytical results for the many-body spectral density.

We will follow the strategy of Mon and French [13] of evaluating moments of the spectral density. In this model, this is again facilitated by noticing that the Euclidean Clifford algebra in $N$ dimensions of the Majorana fermions [Eq. (2)] is shared by Euclidean Dirac $\gamma$ matrices. Therefore, it is possible to employ the full machinery developed in that context to compute the trace of a large number of Majorana fermions, a key part in the calculation of energy moments. We leave the details of the calculation to Appendix B. Here we just define the moments, sketch the main steps of the calculation, and give the final expression as a function of the number of particles $N$. Since the Gaussian disorder distribution is an even function, all odd moments will vanish. From now on, we will focus only on the even ones:

$$M_{2p}(N) = \langle \operatorname{Tr} H^{2p} \rangle, \tag{4}$$

where $p = 1, 2, 3 \ldots$, and $\langle \ldots \rangle$ stands for the spectral and ensemble average. The strategy to evaluate $M_p(N)$ is straightforward: we first perform the Gaussian average, equivalent to summing over all possible contractions according to Wick's theorem, and then we evaluate each of these terms, involving the trace of products of $\gamma$ matrices, by using properties of $\gamma$ matrices in $N$ Euclidean dimensions.

Denoting the product of four $\gamma$ matrices by $\Gamma_\alpha$, we have that the moments are given by

$$M_{2p} = \left\langle \operatorname{Tr} \sum \prod_{k=1}^{2p} J_{\alpha_k} \Gamma_{\alpha_k} \right\rangle. \tag{5}$$

The Gaussian average over the random couplings $J_\alpha$ of the Hamiltonian (1), denoted by $\langle \cdots \rangle$, is equal to the sum over

all possible contractions. In the limit $N \gg 2p$, almost all $\Gamma_\alpha$ have no overlapping indices so that they commute. Because of

$$\Gamma_\alpha^2 = 1, \qquad (6)$$

we find that in this case all $(2p - 1)!!$ contractions give the same contribution, resulting in the moments

$$M_{2p} = (2p - 1)!! \langle J_\alpha^2 \rangle^p 2^{N/2}. \qquad (7)$$

These are the moments of a Gaussian distribution resulting in a Gaussian spectral density. We have evaluated the exact analytical result for $M_4$ and $M_6$. This requires the evaluation of diagrams that are subleading in $N$. For that purpose

it is helpful to note that when we have common $\gamma$ matrices in $\Gamma_\alpha$ and $\Gamma_\beta$, they commute or anticommute depending on the number of common $\gamma$ matrices. This results in large cancellations suppressing the contribution of intersecting diagrams. Following this procedure, the first two nontrivial normalized cumulants, $\kappa_4$ and $\kappa_6$, are easily obtained as a function of $N$ from the moments $M_{2p}(N)$ (see Appendix B for details):

$$\kappa_4(N) = -\frac{32(N - 4)(N^2 - 11N + 36)}{N(N - 1)(N - 2)(N - 3)}, \qquad (8)$$

with large-$N$ asymptotics $-32/N$ and

$$\kappa_6(N) = \frac{512(N - 4)(11N^5 - 304N^4 + 3535N^3 - 21302N^2 + 65856N - 82656)}{(N - 3)^2(N - 2)^2(N - 1)^2N^2}, \qquad (9)$$

with large-$N$ asymptotics $512 \times 11/N^2$, where from now on we set $J = 1$.

For higher moments, the combinatorial problem becomes increasingly difficult, and the final expressions are rather cumbersome. However, these few cumulants already contain interesting information.

As we have seen above, for $N \to \infty$ the normalized cumulants vanish for orders $8p \ll N$. This is a distinctive feature of a Gaussian distribution. Therefore, the average analytical spectral density converges (nonuniformly) to a Gaussian of zero average and variance equal to $6/N^3$.

We note that a Gaussian spectral density is expected for models with an entropy $S = Nf(E/N)$ in the large-$N$ limit. The only requirement is that $f$ must be a smooth function that has a maximum. Gaussian behavior in the central part

of the spectrum, assuming a maximum at $E = 0$, results after expanding $f$ around the maximum.

In Fig. 1, we compare the analytical predictions [Eqs. (8) and (9)] of the normalized fourth and sixth cumulants with numerical results obtained by using exact diagonalization techniques. The agreement is excellent.

In Fig. 2, we depict the average spectral density for $N = 34$, the largest size for which we can obtain numerically the full spectrum, with the analytical prediction of a Gaussian distribution with a variance that has been fitted to the data. Here the agreement is good, but we observe clear deviations in the tail of the density. The reason for that discrepancy is that corrections to the Gaussian distribution, as described by the moments above, are still of order 1 for $N = 34$. We were unable to compute analytically the
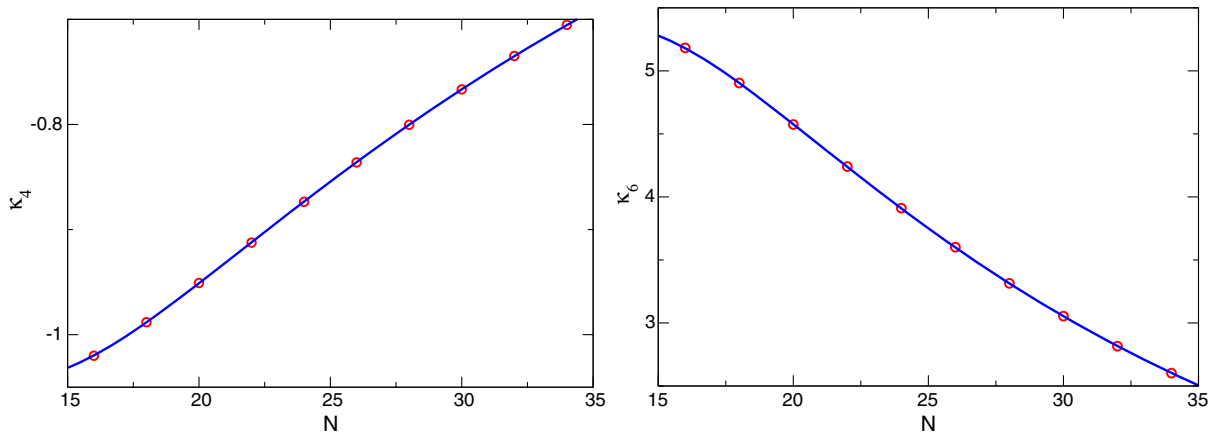


FIG. 1.   The fourth and sixth normalized energy cumulants related to the Hamiltonian (1) as a function of the system size $N$. The circles correspond to the numerical results obtained by exact diagonalization after the spectral and ensemble average. At least a total of $5 \times 10^5$ eigenvalues were employed for each $N$. The solid line is the analytical prediction for the fourth [left; Eq. (8)] and sixth [right; Eq. (9)] cumulant.
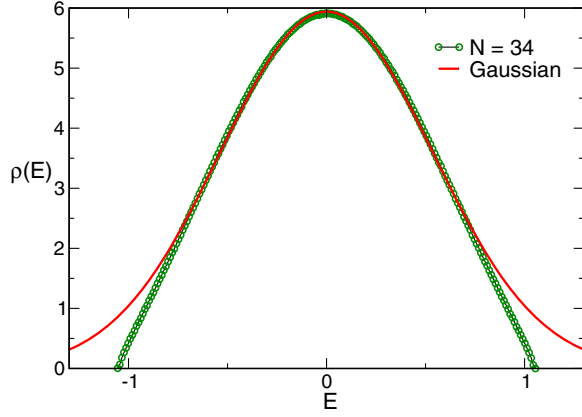
FIG. 2. Spectral density $\rho(E)$ as a function of the energy $E$. The solid line is the analytical prediction valid in the $N \to \infty$ limit. Circles are the numerical spectral density for the largest size $N = 34$ for which we can obtain all eigenvalues of the Hamiltonian. Except for the tails, the agreement with the numerical results is very good.

leading $N$ corrections to the Gaussian density of states. However, in the next section, we carry out a detailed numerical analysis of the tail of the average spectral density.

## III. THERMODYNAMIC PROPERTIES IN THE LOW-TEMPERATURE LIMIT

Part of the renewed interest in the SYK model stems from the fact that its low-temperature properties are similar to those of a gravity background that in the infrared limit is well described by AdS$_2$ geometry. Typical features include a finite entropy at zero temperature, a ground state energy that is extensive in the number of particles, and a specific heat linear in temperature but with a prefactor different from that of free fermions. There are already approximate analytical predictions [21,27] in the literature for these observables. Exact numerical diagonalization of the SYK Hamiltonian [Eq. (1)] was employed in Ref. [21] to compute the zero-temperature entropy [21]. We are not aware of exact diagonalization results for the specific heat or the ground state energy. In this section we address this problem by a detailed numerical study of the tail of the spectrum that controls the thermodynamic properties in the low-temperature limit. We start with the ground state energy. The lowest eigenvalue of the SYK Hamiltonian, $E_{\min}$, is the ground state energy of the SYK model with $N$ Majorana fermions [Eq. (1)]. Due to the fermionic nature of the model, we expect $E_{\min}$ to be proportional to $N$. In Fig. 3 we show the ensemble average of $E_{\min}$ versus $N$, and it indeed shows a nice linear asymptotic dependence on the dimension $N$.

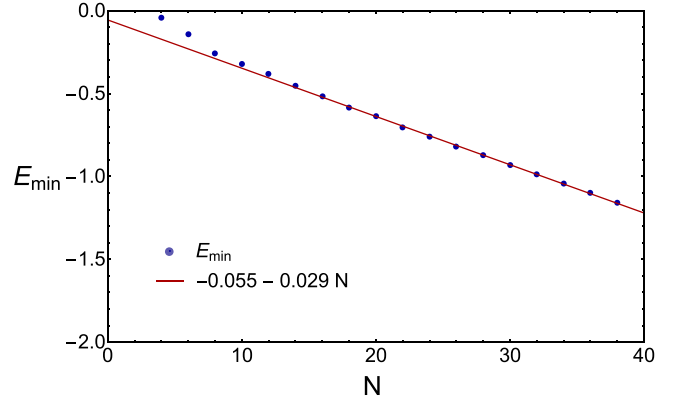From a careful fitting of the numerical data, we find that the tail of the spectrum is well approximated by



FIG. 3. Ensemble average of the smallest eigenvalue as a function of the system size $N$. For $N \gg 1$ we observe that it decreases linearly with $N$. This is an expected feature for a system of $N$ interacting fermions.

$$\rho_{\text{tail}}(E) = 2^{N/2} a (E - E_{\min})^{1/2} [1 + b(E - E_{\min})], \quad (10)$$

which also determines the low-temperature limit of the partition function,

$$Z(\beta) = \int_{E_{\min}}^{\infty} e^{-\beta E} \rho(E),$$
$$\approx \int_{E_{\min}}^{\infty} e^{-\beta E} \rho_{\text{tail}}(E),$$
$$= \frac{a\sqrt{\pi}}{2} \frac{1}{\beta^{3/2}} e^{-\beta E_{\min}} \left(1 + \frac{3}{2\beta} b\right). \quad (11)$$

The low-temperature limit of the SYK model is given by [21,27]

$$Z(\beta) = \frac{c_0}{\beta^{3/2}} e^{-\beta E_0 + S_0 + \frac{c}{2\beta J}}, \quad (12)$$

where the ground state energy $E_0$, the entropy $S_0$, and the specific heat coefficient $c$ are all proportional to $N$. The prefactor $\beta^{-3/2}$ is an order-1 contribution coming from one-loop quantum corrections, and $c_0$ is a temperature-independent constant. Comparing this to Eq. (11), we can make the identification

$$E_0 = E_{\min},$$
$$S_0 = \frac{N}{2} \log 2 + N \frac{d}{dN} \log a. \quad (13)$$

In Fig. 4, we depict $\log a(N)$ and $b(N)$ by the fitting of the exact partition function computed numerically by exact diagonalization. The zero-temperature entropy and the ground state energy are then obtained from Eq. (13):

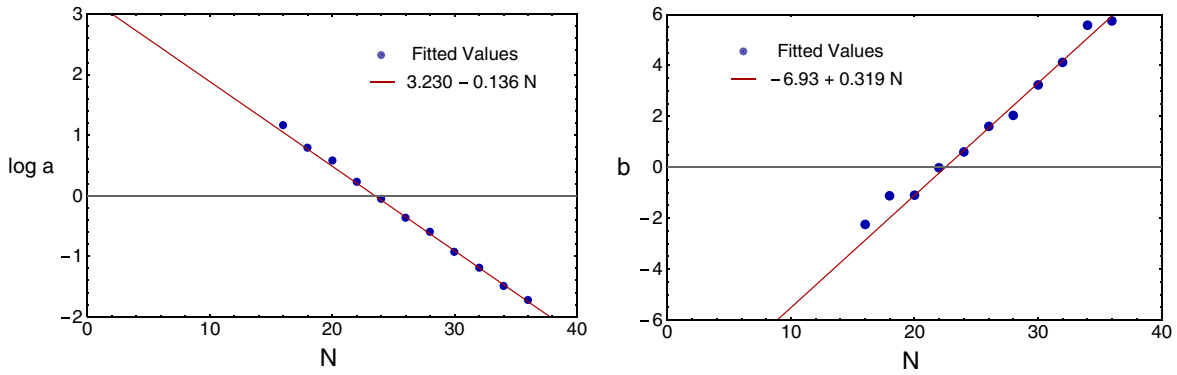$$S_0 = 0.21N, \qquad E_0 = -0.055 - 0.029N. \quad (14)$$

FIG. 4.    The fitted values of $\log a$ (left) and $b$ (right), defined in Eq. (10), versus $N$. The lines are the best fits to the data. In the right figure, only the points for $N \geq 28$ have been used for the fitting.

The value of $S_0$ is in rough agreement with the result $\sim 0.23N$ obtained by Maldacena and Stanford [21].

We now move to the calculation of the specific heat. In the very low-temperature limit with $\beta J \gg N$, we can expand the partition function as

$$Z(\beta) = \frac{c_0}{\beta^{3/2}} e^{-\beta E_0 + S_0} \left[ 1 + \frac{c}{2\beta J} \right]. \qquad (15)$$

It would be tempting to also make the identification

$$\frac{c}{2} = \frac{3}{2} N \frac{db}{dN},$$

but in the parameter range we are looking at, it is not justified to expand the exponential. Rather, we determine the specific heat coefficient $c$ by directly fitting the $\beta$ dependence of the specific heat,

$$\frac{dU(T)}{dT}, \qquad (16)$$

where the internal energy per particle, $U(T)$, is defined in the usual way,

$$U(T) = -\frac{1}{N} \frac{d \log Z}{d\beta}. \qquad (17)$$

Setting $J = 1$ for convenience, and using the low-temperature expansion of the partition function given in Eq. (12),

$$Z(\beta) = \frac{1}{\beta^q} e^{-\beta E_0 + S_0 + \frac{c}{2\beta}}, \qquad (18)$$

we find that

$$\frac{dU}{dT} = \frac{q}{N} + \frac{c}{N} T, \qquad (19)$$

where the exponent $q$ that controls the one-loop quantum correction $1/\beta^q$ to the partition function is left as a free

parameter rather than fixing it to the perturbative [20,21] prediction $q = 3/2$.

In terms of the eigenvalues $E_{k,p}$ of the $p$th member of the ensemble of SYK Hamiltonians, the specific heat per particle is given by

$$\frac{dU(T)}{dT} = \frac{1}{N} \frac{1}{Z} \sum_{k,p} \frac{(E_{k,p} - \langle E \rangle)}{T^2} e^{-\beta E_{k,p}}, \qquad (20)$$

with

$$\langle E \rangle = \frac{1}{Z} \sum_{k,p} E_{k,p} e^{-\beta E_{k,p}} \qquad (21)$$

and

$$Z = \sum_{k,p} e^{-\beta E_{k,p}}. \qquad (22)$$

For a given realization of the random Hamiltonian, the fluctuations of the average energy,

$$\bar{E}_p = \frac{\sum_k E_{k,p} e^{-\beta E_{k,p}}}{\sum_k e^{-\beta E_{k,p}}}, \qquad (23)$$

give rise to significant finite size contributions to the specific heat which can be eliminated by performing the ensemble average relative to the average energy for each realization of the SYK Hamiltonian; i.e.,

$$\frac{dU(T)}{dT} = \frac{1}{N} \frac{1}{Z} \sum_{k,p} \frac{(E_{k,p} - \bar{E}_p)^2}{T^2} e^{-\beta E_{k,p}}. \qquad (24)$$

For a large number of particles, this procedure should be equivalent to the calculation according to Eq. (20). However, for the values of $N$ we work with, this finite size effect must be removed in order to obtain accurate results for the low-temperature limit of the specific heat.
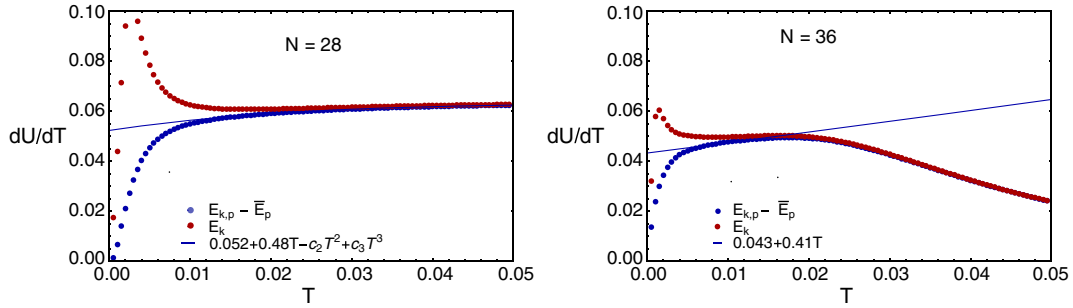
FIG. 5.    The specific heat as a function of the temperature for $N = 28$ (left) and $N = 36$ (right). The red dots represent the numerical result for the SYK model when specific heat is calculated relative to the ensemble average [see Eq. (20)], while the blue dots show the results where the free energy is calculated relative to the average energy $\bar{E}_p$ for each realization of the ensemble [see Eq. (24)]. The blue curve is a linear fit to the blue dots on the interval [0.0075, 0.015] for $N = 36$ and a cubic polynomial fit on [0.025, 0.05] for $N = 28$.

The finite size effects discussed in the previous paragraph decrease rapidly with the total number of particles. As an example, we show in Fig. 5 the temperature dependence of the specific heat for $N = 28$ (left) and $N = 36$ (right). We show both the result where the specific heat is calculated according to Eq. (20) (red dots) and the result where we first calculate the specific heat for each realization of the Hamiltonian and then perform the ensemble average as given in Eq. (24) (blue dots). The curves are fits to the blue dots.

Except for $N = 36$, where we have only 2000 eigenvalues for each configuration and use a linear fit on a shorter fitting interval, we use cubic fits

$$\frac{dU(T)}{dT} = \frac{q(N)}{N} + c(N)T + c_2(N)T^2 + c_3(N)T^3. \quad (25)$$

In Fig. 6, we show the $N$ dependence of $q(N)$ (left) and $c(N)$ (right), which are fitted by a constant for $N \geq 28$ (see curves). This results in the following estimates for the exponent $q$ in Eq. (18) that controls one-loop quantum corrections and the specific heat coefficient:

$$q = 1.53 \pm 0.2, \qquad c/N = 0.43 \pm 0.10. \quad (26)$$

The value of $q$ is consistent with the estimate $q = 3/2$ [21] from an analytical calculation of one-loop quantum corrections to the classical action. It is also in agreement with the semicircular form of the spectral density, see Eq. (10). Likewise, the analytical estimation of the specific heat coefficient $c/N = 0.396$ [21] is also consistent with our numerical results.

We note that all the results of this section are based on the ansatz Eq. (10) for the density of states. The exponent $1/2$ of the prefactor was chosen because it gave the best fit to the numerical results. However, there is an indirect theoretical justification for that exponent. In the recent literature on the SYK model, there are several studies [20–22,27] of the one-point temporal correlation function, which is the Fourier transform of the strength function

$$-\frac{1}{N}\sum_\alpha \sum_k |\langle 0|\gamma_\alpha|k\rangle|^2 \delta(E + E_k - E_0), \quad (27)$$

where $E_0$ is the $N$-particle ground state energy, $|k\rangle$ are eigenstates with $N \pm 1$ particles, and $\gamma_\alpha$ is a Euclidean $\gamma$ matrix. These results are based on perturbative semiclassical techniques that typically are valid only up to time scales of the order of the Ehrenfest time. However, in Ref. [28], a nonperturbative treatment of quasizero modes enlarged the
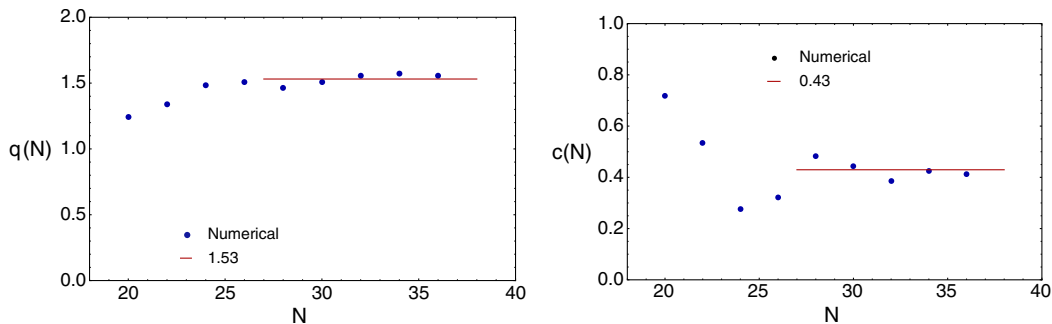


FIG. 6.    The exponent of the prefactor $\beta^{-q(N)}$ of the partition function [Eq. (18)] versus $N$ (left) and the specific heat coefficient $c(N)$ [Eq. (25)] versus $N$ (right). The exponent $q(N)$ and the specific heat coefficient $c(N)$ are fitted by a constant.

time domain of applicability of the analytical results to scales shorter than, but of the order of, the Heisenberg time. Interestingly, it was found [28] that, in an energy representation, the strength function for low energies $\propto \sqrt{E - E_0}$. In principle, the strength function is unrelated to the many-body spectral density Eq. (10) because the former also provides information of the correlations between eigenvalues and eigenvectors. However, if the eigenvectors and the eigenvalues are uncorrelated, as is the case for the Wigner-Dyson random matrix ensembles, the strength function is proportional to the spectral density. Below, we will see that spectral correlations of the SYK model are well described by the Wigner-Dyson ensembles, which justifies *a posteriori* the ansatz in Eq. (10) for the tail of the spectral density.

In summary, we have shown that the spectral density of the SYK model is Gaussian in the limit of a large number of particles $N$, so it is qualitatively different from the semicircle law typical of random matrices. However for a fixed finite $N$, the tail of the spectral density is close to a semicircle law, while the center is Gaussian. The value of the zero-temperature entropy and specific heat coefficient, obtained numerically from the tail of the spectrum and the low-temperature behavior of the partition function, are close to previously obtained analytical estimates [21,27].

## IV. SPECTRAL CORRELATIONS

In this section we investigate eigenvalue correlations that provide valuable information on the dynamics of the system. We focus on long time scales of the order of the Heisenberg time $\sim \hbar / \Delta$, where $\Delta$ is the mean level spacing. Disordered metals, or quantum chaotic systems, are expected to be described by the invariant random matrix ensembles in this region. Physically, agreement with random matrix theory predictions indicates that an initially localized wave packet reaches the boundary of the sample for sufficiently long time scales. For a disordered insulator, we expect level correlations to be described by Poisson statistics. Although in the literature on $k$-body embedded fermionic ensembles there are some reports of Poisson statistics for two-body random interactions in the dilute limit [42], there is broad evidence from numerical and analytical findings [10,14,43] that level statistics are very close to the random matrix theory prediction, at least for short-range eigenvalue correlations.

As was mentioned in the Introduction, the only previous study of spectral correlations in the SYK model [30] investigated numerically the ratio of consecutive level spacings, which only explores time scales of the order of the Heisenberg time. For shorter time scales, corresponding to energy scales beyond the mean level spacing, level statistics for the SYK model are yet an open problem. We shall see that level statistics in this region are well described by random matrix theory, though deviations, that decrease with $N$, are systematically observed for larger

spectral distances corresponding to time scales much shorter than the Heisenberg time.

The universality class for the spectral correlations is determined by the antiunitary and involutive symmetries of the system. Since the SYK Hamiltonian does not have any involutive symmetries, the universality class is given by the Wigner-Dyson random matrix ensembles with a Dyson index $\beta_D = 1$, 2 or 4. The first case is when the antiunitary symmetry squares to 1, the second case when there are no antiunitary symmetries, and the third case when the antiunitary symmetry squares to $-1$. The SYK Hamiltonian has two antiunitary symmetries (see Table I),

$$[C_1 K, H_{\mathrm{SYK}}] = 0, \qquad [C_2 K, H_{\mathrm{SYK}}] = 0, \qquad (28)$$

which is equivalent to one irreducible antiunitary symmetry, $C_1 K$, and the unitary symmetry $C_1 K C_2 K$. Physically, the symmetries $C_1 K$ and $C_2 K$ are charge conjugation symmetries which are equal to the product of the "even" gamma matrices or "odd" gamma matrices, respectively (choosing the right labeling for "even" and "odd"). Therefore, $C_1 K C_2 K \sim \Gamma_5$, with $\Gamma_5 = \mathrm{diag}(1, …, 1, -1, …, -1)$ in a chiral representation of the Dirac $\gamma$ matrices. In this representation the SYK Hamiltonian splits into two diagonal block matrices of equal size. If $C_1 K C_2 K = \pm \Gamma_5$, the charge conjugation matrix commutes with the projection on the diagonal blocks. If $(C_1 K)^2 = 1$, it is possible [44] to find an $H$-independent basis for which the blocks become real, corresponding to a Dyson index $\beta_D = 1$. Moreover, if $(C_1 K)^2 = -1$, it is possible to construct an $H$-independent basis for which the Hamiltonian can be arranged into quaternion real matrix elements corresponding to a Dyson index $\beta_D = 4$. If $C_1 K C_2 K = \pm i \Gamma_5$, the charge conjugation matrix does not commute with the projection onto the blocks. Therefore, we cannot use these symmetries to construct a basis for which the Hamiltonian becomes real or quaternion real. Since there are no unitary symmetries, the matrix elements of the SYK Hamiltonian are complex, corresponding to a Dyson index $\beta_D = 2$. However, the symmetry $C_1 K$ still can be used to show that both blocks have the same eigenvalues (see Ref. [45] for a similar reasoning). We refer to Appendix A for all technical details.

TABLE I. (Anti-)unitary symmetries of the SYK Hamiltonian and the corresponding random matrix ensemble. The symmetries are periodic in $N$ modulo 8.

| $N$ | $(C_1 K)^2$ | $(C_2 K)^2$ | $C_1 K C_2 K$ | RMT |
|---|---|---|---|---|
| 2 | 1 | $-1$ | $-i\Gamma_5$ | GUE |
| 4 | $-1$ | $-1$ | $-\Gamma_5$ | GSE |
| 6 | $-1$ | 1 | $-i\Gamma_5$ | GUE |
| 8 | 1 | 1 | $\Gamma_5$ | GOE |
| 10 | 1 | $-1$ | $-i\Gamma_5$ | GUE |
| 12 | $-1$ | $-1$ | $\Gamma_5$ | GSE |

For our study, we employ the level spacing distribution $P(s)$ [Eq. (29)], the probability to find two neighboring eigenvalues separated by a distance $s = (E_{i+1} - E_i)/\Delta$, and the number variance $\Sigma^2(L)$ [Eq. (31)], that describes fluctuations in the number of eigenvalues in a spectral window of size $L$, again measured in units of the mean level spacing $\Delta$. The latter, a long-range spectral correlator directly related to the two-point correlation function, gives information on the quantum dynamics for time scales of the order of, but much larger than, the mean level spacing (Heisenberg time). We shall use it to investigate deviations from random matrix predictions. The former is more suited to study longer time scales $\approx \hbar/\Delta$ and also provides indirect information on higher-order correlation functions.

We investigate level statistics numerically by an exact diagonalization of the upper block of the Hamiltonian (1) for $N \leq 36$. The first step in the spectral analysis is the unfolding of the spectrum [7]—namely, to rescale the spectrum so that the mean level spacing is the same for all energies. This is a necessary condition to compare level statistics in different parts of the spectrum. For that purpose, for each $N$, we employ the averaged smooth staircase function (the integral of the spectral density) resulting from a fifth-order polynomial fitting involving only odd powers to unfold the spectrum. The spectrum rescaled in that way, which has unit mean level spacing for all energies, is ready for the level statistics analysis. We have observed that level statistics are similar for all energies. Except for $N = 36$, where we have only obtained about 2% of eigenvalues close to the edge of the spectrum, we have taken about 70% of the eigenvalues around $E \approx 0$.

### A. Short-range spectral correlations: $P(s)$

The level spacing distribution $P(s)$ is the probability to find two eigenvalues separated at a distance $s$ in units of $\Delta$ with no other eigenvalues in between:

$$P(s) = \sum_i \langle \delta(s - \epsilon_i + \epsilon_{i+1}) \rangle \quad \epsilon_i = E_i/\Delta. \quad (29)$$

In an insulator, it is given by Poisson statistics: $P(s) = e^{-s}$. By contrast, the random matrix prediction, which applies to a disordered metal and to a quantum chaotic system, is very well approximated by the Wigner surmise,

$$P(s) \approx a_\beta s^\beta \exp(-b_\beta s^2). \quad (30)$$

Level repulsion, $P(s) \to 0$ for $s \to 0$, is a distinguishing feature of extended states, though its strength depends on the global symmetries of the Hamiltonian (1). For systems that admit a real representation of the Hamiltonian, due to time reversal invariance (or more generally, due to an antiunitary symmetry that squares to 1), $\beta = 1$, $a_1 = \pi/2$, $b_1 = \pi/4$. Similarly, if the Hamiltonian only admits a complex representation, due for instance to the breaking
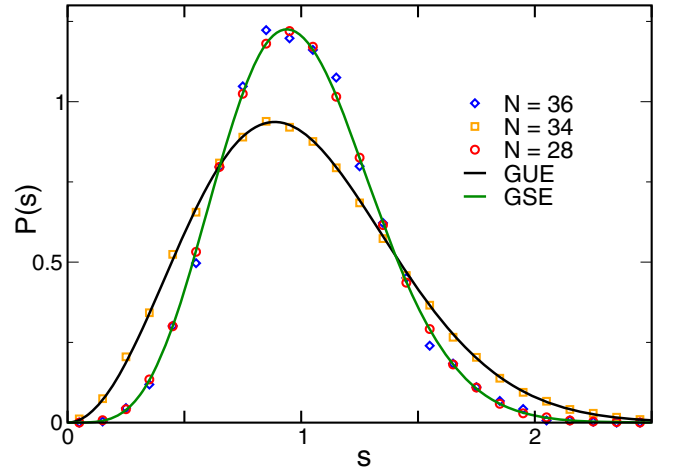


FIG. 7. Level spacing distribution $P(s)$ [Eq. (29)]. Numerical results $N = 28$ (circles), $N = 34$ (squares), and $N = 36$ (diamonds) are in excellent agreement with the predictions of random matrix theory (solid lines) corresponding to the Gaussian unitary ensemble (GUE) for $N = 34$ and the Gaussian symplectic ensemble (GSE) for $N = 28, 36$. We note that while for $N = 28, 34$ we have taken about 70% of the available spectrum around the center of the band; for $N = 36$, where we cannot diagonalize the full Hamiltonian, we consider only a total of about 15000 different eigenvalues close to the ground state from 15 disorder realizations. The universality class is controlled by the type of allowed representations of the Clifford algebra of the Majorana fermions, which is sensitive to $N$ (see Table I and the main text for more details). These results clearly show that the SYK model has quantum chaotic features even for large times $s \sim 1$ of the order of the Heisenberg time.

of time translational invariance as a consequence of a magnetic field or flux, $\beta = 2$, $a_2 = 32/\pi^2$, $b_2 = 4/\pi$. Finally, the case $\beta = 4$, $a_4 = 262144/729\pi^3$, $b_4 = 64/9\pi$ corresponds to systems with time reversal symmetry and strong spin-orbit interactions leading to a doubly degenerate spectrum (or more generally, to systems with an antiunitary symmetry that squares to $-1$). It is typical of random matrices with quaternionic entries.

In Fig. 7, we plot $P(s)$ for $N = 28$, $N = 34$ and $N = 36$. Excellent agreement with the random matrix prediction is found in all cases. As can be seen from Table I, $N = 28$ belongs to the Gaussian symplectic ensemble (GSE) universality class ($\beta_D = 4$), while $N = 34$ belongs to the Gaussian unitary ensemble (GUE) universality class ($\beta_D = 2$). We note that the $N$ dependence of the universality class was already reported in Ref. [30], although it was not discussed that this was a simple consequence of two features of Clifford algebras: the existence of real, complex or quaternionic representations for different values of the dimensionality $N$ and Bott periodicity—namely, these representations follow a periodic pattern; in this case the Bott periodicity is $N$ mod 8. An example of a period is $N = 36$: GSE; $N = 34$: GUE; $N = 32$: GOE; $N = 30$: GUE; and so on.
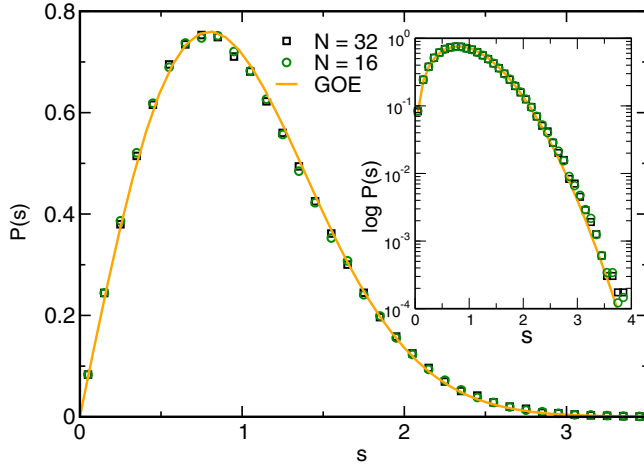
FIG. 8. Level spacing distribution $P(s)$ [Eq. (29)], for $N = 16$ (circles) and $N = 32$ (squares). For both dimensions, the Clifford algebra admits a real representation so the expected universality class is that of the Gaussian orthogonal ensemble (GOE). Indeed, the numerical results (symbols) are in excellent agreement with the GOE prediction. Interestingly, despite the vast difference in size, we do not observe substantial deviations from the GOE prediction, even for $N = 16$, where mesoscopic fluctuations are expected to be stronger.

In Fig. 8, we depict $P(s)$ for $N = 16$ and $N = 32$ both belonging to the Gaussian orthogonal ensemble (GOE) universality class. Despite the large difference in size, we do not observe important differences between the two cases. We will see in the following analysis of the number variance, a long-range spectral correlator, that deviations from random matrix theory eventually occur for larger eigenvalue separations, which indicates that the SYK model is not ergodic for sufficiently short time scales.

## B. Long-range spectral correlations: The number variance $\Sigma^2(L)$

The number variance is defined as the variance of the number of levels $N$ inside an energy interval that has (in units of the mean level spacing) $L$ eigenvalues on average:

$$\Sigma^2(L) = \langle N^2(L) \rangle - \langle N(L) \rangle^2. \tag{31}$$

For a Poisson distribution typical of an insulator, different parts of the spectrum are not correlated, so the number variance is linear with slope 1, $\Sigma^2(L) = L$. The random matrix prediction, that also occurs in noninteracting [39,40] and strongly coupled [41] disordered metals below the Thouless energy, is that level repulsion causes, for $L \gg 1$, a slow logarithmic increase, usually termed the *level or spectral rigidity* of the number variance:

$$\Sigma^2(L) \approx c_\beta(\log(d_\beta \pi L) + \gamma + 1 + e_\beta \ldots), \tag{32}$$
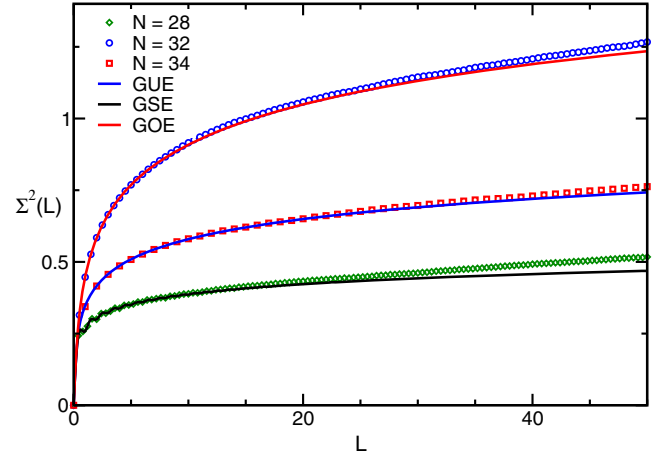


FIG. 9. Number variance $\Sigma^2(L)$ [Eq. (31)], for $N = 28$ (diamonds), $N = 32$ (circles), $N = 34$ (squares), which belong to the GSE, GOE and GUE universality classes, respectively (solid lines), as a function of the width $L$ of the energy interval, corresponding to a spectral window with $L$ eigenvalues on average. For sufficiently large $L$, we start observing deviations from the random matrix theory predictions.

with $c_1 = 2/\pi^2$, $c_2 = c_1/2$, $c_4 = c_1/4$, $d_1 = d_2 = 2$, $d_4 = 4$, $e_1 = -\pi^2/8$, $e_2 = 0$, $e_4 = \pi^2/8$, and where $\gamma = 0.5772\ldots$ is Euler's constant. In Fig. 9, we depict the number variance for several values of the system size, $N = 28$, $N = 32$ and $N = 34$, each of them belonging to a different universality class: GOE for $N = 32$, GUE for $N = 34$, and GSE for $N = 28$. For all universality classes we find an excellent agreement with the random matrix prediction for small $L$. However, we observe systematic deviations for sufficiently large $L \gtrsim 30$. As $N$ increases, the region of agreement with random matrix increases as well—namely, deviations are observed only for larger $L$.

In Fig. 10, we depict the number variance for two sizes ($N = 22$ and $N = 34$) belonging to the same universality, but one matrix size is much smaller than the other. The idea is to study finite size effects related to mesoscopic fluctuations in the number variance. For small $L \leq 20$, the number variance follows the GUE prediction for both sizes. However, for larger $L$, deviations from the random matrix result occur much earlier, and grow much faster, for $N = 22$ than for $N = 34$. An eyeball estimate suggests that the region of agreement with random matrix predictions scales approximately as $2^{N/8}$.

Several conclusions can be drawn from these results: (a) The SYK model has spectral correlations similar to that of a disordered metal or a quantum chaotic systems even for energy scales much larger than the inverse mean level spacing. (b) Deviations for sufficiently large scales suggest that, unlike a dense random matrix, the SYK model is not ergodic for sufficiently short time scales. This is expected, as the Hamiltonian is rather sparse, with only $\sim N^4$ nonzero elements. This feature is also required for a gravity-dual
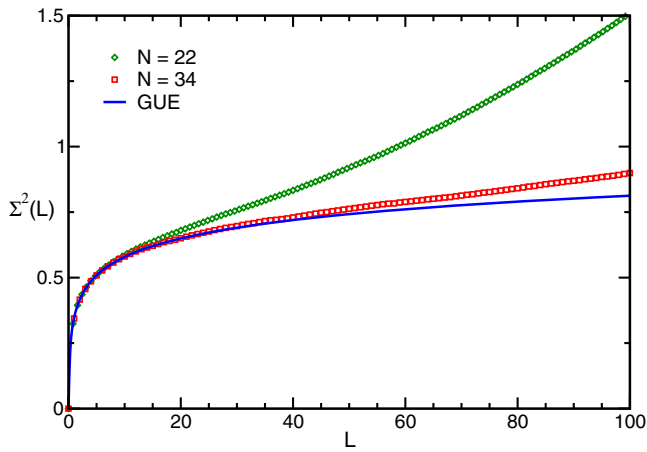
FIG. 10. Number variance $\Sigma^2(L)$ [Eq. (31)], for $N = 22$ and $N = 34$, both corresponding to the GUE universality classes. We observe that deviations from the random matrix prediction occur much earlier for the smaller dimension $N = 22$. This suggests that the observed deviations are due to mesoscopic fluctuations in a way reminiscent to the existence of a Thouless energy in the system. It is also an indication that the system is not ergodic and chaotic for sufficiently short times, an expected feature [20,46] in field theories with a gravity dual.

interpretation, where it is expected that, for times of the order of the Ehrenfest time $\sim \log 1/\hbar$, certain correlation functions grow exponentially at a rate controlled by the Lyapunov exponent of the system [37]. (c) The fact that as $N$ increases, deviations from the random matrix occur for larger $L$ is a strong indication that the observed chaotic features persist in the thermodynamic limit. It also suggests the existence of the equivalent of a Thouless energy in the system related to the typical time necessary to explore the full available phase space.

## V. OUTLOOK AND CONCLUSIONS

We have shown analytically that, in the limit of a large number of particles, the SYK Hamiltonian has a Gaussian spectral density, although for a fixed finite number of particles, we have found numerically that the tail of the density is well approximated by the semicircle law. Level statistics are well described by random matrix theory up to energy scales much larger than, but still of the order of, the mean level spacing. Deviations from random matrix theory for larger energies, or shorter times, are an indication that the model is not ergodic for short times. Together with previous results, this is a further confirmation that the SYK model has quantum chaotic features at any time scale. According to Ref. [21], this is an expected feature in field theories with a gravity dual. Indeed, we have numerically calculated the specific heat and the entropy, and found that the low-temperature thermodynamic properties of the SYK model are similar to those of a gravity background with an AdS$_2$ infrared limit. To some extent, our work on the SYK

model shows that a compound nucleus may have a gravity dual.

Finally, we mention a few venues for further research. It would be interesting to explore metal-insulator transitions in the model by reducing the range of the interaction from infinity to a power-law decay. Another interesting problem is to evaluate analytically the two-level correlation function in the $N \to \infty$ limit by the replica trick by following the procedure of Ref. [14] for the $k$-body embedded ensemble. Similarly, the analytical evaluation of the leading finite $N$ corrections of the spectral density, by a careful evaluation of higher-order $N$ moments, would provide a full description of the low-temperature thermodynamic properties of the model. This is a necessary step for a full understanding of the relevance of the SYK model in holography. We plan to address some of these problems in future publications.

*Note added in proof.*—After this paper was accepted for publication, a paper [47] appeared that also studies thermodynamic and spectral properties in the SYK model. In this paper spectral correlations are investigated [47] by means of correlators of partition functions which at infinite temperature reduce to the spectral form factor which is the Fourier transform of the two-point correlation function.

## APPENDIX A: CONSTRUCTION OF THE GAMMA MATRICES

The $\gamma$ matrices are constructed iteratively starting from the gamma matrices in two dimensions:

$$\gamma_1^{(2)} = \sigma_1, \qquad \gamma_2^{(2)} = \sigma_2, \qquad \gamma_3^{(2)} = \sigma_3, \qquad \text{(A1)}$$

and using the recursion relation

$$\gamma_k^{(d+2)} = \sigma_1 \otimes \gamma_k^d, \quad \text{for } k = 1, \dots, d+1,$$
$$\gamma_{d+2}^{(d+2)} = \sigma_2 \otimes 1_{2^{d/2}} \qquad \text{(A2)}$$

to extend it to $d + 2 = N$ dimensions, where $N$ is an even number of Majorana fermions. As we will see below, in this

representation, the product of four gamma matrices is block diagonal.

We can construct two antiunitary symmetry operators (note that the gamma matrices in $C_1$ are purely imaginary, while the $\gamma$ matrices in $C_2$ are purely real):

$$C_1 = \gamma_1 \prod_{i=2}^{N} \gamma_{2i} K,$$

$$C_2 = \gamma_2 \prod_{i=2}^{N-1} \gamma_{2i+1} K, \tag{A3}$$

where $K$ is the complex conjugation operator (we could have interchanged the labels of $\gamma_1$ and $\gamma_2$ so that $C_1$ would have been the product of the odd gamma matrices and $C_2$ the product of the even gamma matrices). They satisfy the symmetry relations

$$C_1 K \gamma_\mu + (-1)^{N/2} \gamma_\mu C_1 K = 0,$$
$$C_2 K \gamma_\mu - (-1)^{N/2} \gamma_\mu C_2 K = 0, \tag{A4}$$

with $\mu = 1, \ldots N$. Since the Hamiltonian is a sum of products of four gamma matrices, we have

$$[C_1 K, H] = 0, \qquad [C_2 K, H] = 0. \tag{A5}$$

We also have that

$$[C_1 K, C_2 K] = 0. \tag{A6}$$

In Table I given in the main text, we give the main properties of these antiunitary symmetries. Because of (A5), we have that $[\Gamma_5, H] = 0$, with $\Gamma_5 = i^{-N/2} \prod_{i=1}^{N} \gamma_i$, so that $H$ splits into two block-diagonal matrices of the same size. If $C_1 K C_2 K = \pm \Gamma_5$, then

$$P \equiv \frac{1}{2}(1 + C_1 K C_2 K) \tag{A7}$$

is a projection operator

$$P^2 = P, \tag{A8}$$

and

$$[P, H] = 0, \qquad [C_1 K, P] = 0. \tag{A9}$$

In this case we have that $(C_1 K)^2 = (C_2 K)^2 = \pm 1$. If $(C_1 K)^2 = 1$, it is possible to find an $H$-independent basis in which $H$ becomes real, and the corresponding random matrix ensemble is the Gaussian orthogonal ensemble (GOE). If $(C_1 K)^2 = -1$, the Hamiltonian is a self-dual quaternion up to an $H$-independent unitary transformation which corresponds to the Gaussian symplectic ensemble. In this case, the eigenvalues of $H$ are a multiple of the quaternion identity and are thus doubly degenerate.

If $C_1 K C_2 K = \pm i \Gamma_5$, the projection operator is given by

$$P_i = \frac{1}{2}(1 \pm i C_1 K C_2 K), \tag{A10}$$

and

$$[P_i, H] = 0, \tag{A11}$$

but because of the $i$, this projection operator does not commute with $C_1 K$ or $C_2 K$. So there are no antiunitary symmetries when $H$ is block diagonal, and we are in the universality class of the Gaussian unitary ensemble. In this case, the charge conjugation matrices anticommute with $\gamma_5$,

$$\{C_1, \Gamma_5\} = 0, \qquad \{C_2, \Gamma_5\} = 0, \tag{A12}$$

so that $C_1$ and $C_2$ are block off-diagonal,

$$C_1 K = \begin{pmatrix} 0 & c_1 K \\ c_1^* K & 0 \end{pmatrix}, \qquad C_2 K = \begin{pmatrix} 0 & c_2 K \\ c_2^* K & 0 \end{pmatrix}, \tag{A13}$$

with $c_{1,2}^* c_{1,2} = -1$. If

$$H = \begin{pmatrix} A & 0 \\ 0 & B \end{pmatrix}, \tag{A14}$$

then the antiunitary symmetries (A5) result in the relation

$$B^* = -c_i^* A c_i, \qquad i = 1, 2. \tag{A15}$$

Because $A$ and $B$ are Hermitian and $c_i^* c_i = -1$, we find from the secular equation that $A$ and $B$ have the same eigenvalues.

## APPENDIX B: CALCULATION OF THE FOURTH AND SIXTH CUMULANTS

In this appendix, we calculate the normalized fourth and sixth cumulants for the Hamiltonian of the SYK model.

### 1. The fourth-order cumulant

The normalized fourth cumulant is given by

$$\kappa_4 = \frac{M_4(N)}{M_2^2(N)} - 3. \tag{B1}$$

We now proceed to the calculation of $M_4(N)$. The Gaussian average is the sum over all pairwise contractions. Because $\Gamma_\alpha^2 = 1$, with $\Gamma_\alpha$ a product of four different gamma matrices, we find that the nested contractions are given by
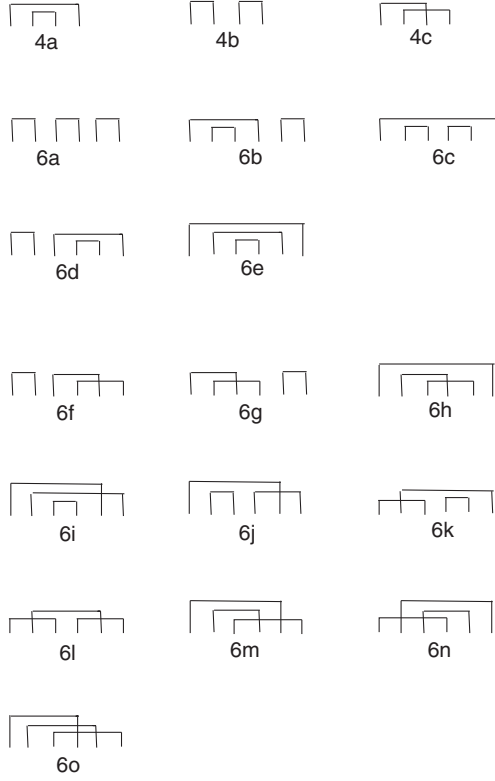
$$2M_2^2(N), \tag{B2}$$

FIG. 11. Contractions contributing to the fourth- and sixth-order cumulants.

with the factor 2 corresponding to the two contractions 4a and 4b in Fig. 11. For the intersecting contraction (see Fig. 11, diagram 4c), we have to evaluate the trace

$$\mathrm{Tr}\sum_{\alpha\beta}\Gamma_\alpha\Gamma_\beta\Gamma_\alpha\Gamma_\beta. \tag{B3}$$

We have that

$$\Gamma_\alpha\Gamma_\beta = (-1)^q\Gamma_\beta\Gamma_\alpha, \tag{B4}$$

with $q$ the number of gamma matrices that $\alpha$ and $\beta$ have in common. For the sum over $\alpha$ and $\beta$, we thus obtain (see diagram 4c) in Fig. 11

$$T_{4c} = M_2^2(N)\binom{N}{4}^{-1}\sum_{q=0}^{4}(-1)^q\binom{N-4}{4-q}\binom{4}{q}. \tag{B5}$$

Note that, as a check of this result, without the factor $(-1)^q$, the sum over $q$ just gives $\binom{N}{4}$. The result $T_{4c}$ can be simplified to

$$T_{4c} = M_2^2(N)\frac{N^4 - 38N^3 + 491N^2 - 2566N + 4608}{N(N-1)(N-2)(N-3)}. \tag{B6}$$

This results in the normalized fourth-order cumulant

$$\kappa_4(N) = \frac{T_{4c}}{M_2^2(N)} - 1$$

$$= -\frac{32(N-4)(N^2 - 11N + 36)}{N(N-1)(N-2)(N-3)}. \tag{B7}$$

### 2. The sixth-order cumulant

In this subsection, we evaluate the normalized sixth-order cumulant, which in terms of the moments is given by

$$\kappa_6 = \frac{M_6(N)}{M_2^3(N)} - 15\frac{M_4(N)}{M_2^2(N)} + 30. \tag{B8}$$

Since $M_4(N)$ was computed in the previous section, we focus on $M_6(N)$. The Gaussian integral for the sixth moment is again evaluated by summing over all pairwise contractions. In this case, there are fifteen diagrams, and five of them are nested; see Fig. 11, diagrams 6a–6e. The nested diagrams are simply given by $M_2^3(N)$. The next simplest class of diagrams are those where two neighboring Hamiltonians are contracted, while the contractions of the remaining factors are intersecting; see Fig. 11, diagrams 6f–6k. Their contribution to the sixth moment is given by

$$T_{6f} = T_{6g} = T_{6h} = T_{6i} = T_{6j} = T_{6k} = M_2(N)T_{4c}. \tag{B9}$$

By a cyclic permutation of the factors in $\mathrm{Tr}H^6$, it is clear that diagrams 6l–6n in Fig. 11 are the same. If we fix the index of the second factor in diagram 6l, it is clear that by commuting the factors as

$$\Gamma_\alpha\Gamma_\beta\Gamma_\alpha\Gamma_\gamma\Gamma_\beta\Gamma_\gamma \to \Gamma_\alpha\Gamma_\alpha\Gamma_\beta\Gamma_\beta\Gamma_\gamma\Gamma_\gamma, \tag{B10}$$

we obtain the same combinatorial factor for the sum over $\alpha$ and $\gamma$ as in diagram 4c. We thus find

$$T_{6l} = T_{6m} = T_{6n} = M_2^3(N)\binom{N}{4}^{-2}$$

$$\times \left[\sum_{q=0}^{4}(-1)^q\binom{N-4}{4-q}\binom{4}{q}\right]^2. \tag{B11}$$

The most complicated diagram is diagram 6o, corresponding to the trace

$$\mathrm{Tr}[\Gamma_\alpha\Gamma_\beta\Gamma_\gamma\Gamma_\alpha\Gamma_\beta\Gamma_\gamma]. \tag{B12}$$

The simplest way to do combinatorics is to think of $\Gamma_\beta\Gamma_\gamma$ as a product of eight gamma matrices with $q$ gamma matrices in common, while $\Gamma_\alpha$ share $l$ gamma matrices with $\Gamma_\beta\Gamma_\gamma$, and of those $l$ there are $l - m$ in the common factors. The result for this diagram is given by

$$T_{6o} = M_2^3(N) \binom{N}{4}^{-2} \sum_{q=0}^{4} \sum_{l=0}^{4} \sum_{m=0}^{l} (-1)^{q+m} \binom{N-8+q}{4-l} \binom{8-2q}{m} \binom{N-4}{4-q} \binom{4}{q} \binom{q}{l-m}. \tag{B13}$$

Again, as a check of this result, if the phase factor $(-1)^{q+m}$ is set to 1, we find $M_2^3(d)$.

Combining all contributions, we find the normalized sixth cumulant:

$$\kappa_6(N) = \frac{512(N-4)(11N^5 - 304N^4 + 3535N^3 - 21302N^2 + 65856N - 82656)}{(N-3)^2(N-2)^2(N-1)^2 N^2}. \tag{B14}$$

[1] E. Wigner, *Math. Proc. Cam. Phil. Soc.* **49**, 790 (1951).
[2] F. Dyson, J. Math. Phys. (N.Y.) **3**, 140 (1962).
[3] F. Dyson, J. Math. Phys. (N.Y.) **3**, 157 (1962).
[4] F. Dyson, J. Math. Phys. (N.Y.) **3**, 166 (1962).
[5] F. Dyson, J. Math. Phys. (N.Y.) **3**, 1191 (1962).
[6] F. Dyson, J. Math. Phys. (N.Y.) **13**, 90 (1972).
[7] T. Guhr, A. Mueller-Groeling, and H. A. Weidenmueller, Phys. Rep. **299**, 189 (1998).
[8] H. A. Bethe, Phys. Rev. **50**, 332 (1936).
[9] O. Bohigas and J. Flores, Phys. Lett. **34B**, 261 (1971).
[10] O. Bohigas and J. Flores, Phys. Lett. B **35B**, 383 (1971).
[11] J. French and S. Wong, Phys. Lett. **33B**, 449 (1970).
[12] J. French and S. Wong, Phys. Lett. **35B**, 5 (1971).
[13] K. Mon and J. French, Ann. Phys. (N.Y.) **95**, 90 (1975).
[14] J. Verbaarschot and M. Zirnbauer, Ann. Phys. (N.Y.) **158**, 78 (1984).
[15] L. Benet and H. A. Weidenmller, J. Phys. A **36**, 3569 (2003).
[16] J. Gomez, K. Kar, V. Kota, R. Molina, A. Relano, and J. Retamosa, Phys. Rep. **499**, 103 (2011).
[17] T. A. Brody, J. Flores, J. B. French, P. A. Mello, A. Pandey, and S. S. M. Wong, Rev. Mod. Phys. **53**, 385 (1981).
[18] V. K. B. Kota, *Embedded Random Matrix Ensembles in Quantum Physics*, Vol. 884 (Springer, New York, 2014).
[19] V. K. B. Kota, A. Relao, J. Retamosa, and M. Vyas, J. Stat. Mech. (2011), P10028.
[20] A. Kitaev, A Simple Model of Quantum Holography, in KITP Strings Seminar and Entanglement 2015 Program, 2015, http://online.kitp.ucsb.edu/online/entangled15/.
[21] J. Maldacena and D. Stanford, Phys. Rev. D **94**, 106002 (2016).
[22] J. Polchinski and V. Rosenhaus, J. High Energy Phys. 04 (2016) 001.
[23] J. Engelsöy, T. G. Mertens, and H. Verlinde, J. High Energy Phys. 07 (2016) 139.
[24] A. Almheiri and J. Polchinski, J. High Energy Phys. 11 (2015) 014.
[25] J. M. Magán, Phys. Rev. Lett. **116**, 030401 (2016).
[26] I. Danshita, M. Hanada, and M. Tezuka, arXiv:1606.02454.
[27] A. Jevicki, K. Suzuki, and J. Yoon, J. High Energy Phys. 07 (2016) 007.
[28] D. Bagrets, A. Altland, and A. Kamenev, Nucl. Phys. **B911**, 191 (2016).
[29] S. Sachdev, Phys. Rev. X **5**, 041025 (2015).
[30] Y.-Z. You, A. W. Ludwig, and C. Xu, arXiv:1602.06964.
[31] D. J. Gross and V. Rosenhaus, arXiv:1610.01569.
[32] L. García-Álvarez, I. L. Egusquiza, L. Lamata, A. del Campo, J. Sonner, and E. Solano, arXiv:1607.08560.
[33] S. Sachdev and J. Ye, Phys. Rev. Lett. **70**, 3339 (1993).
[34] J. Maldacena, Int. J. Theor. Phys. **38**, 1113 (1999).
[35] K. Jensen, Phys. Rev. Lett. **117**, 111601 (2016).
[36] M. Cveti and I. Papadimitriou, arXiv:1608.07018.
[37] J. Maldacena, S. H. Shenker, and D. Stanford, J. High Energy Phys. 08 (2016) 106.
[38] E. Witten, arXiv:1610.09758.
[39] B. Altshuler, I. Zarekeshev, S. Kotochigova, and B. Shklovskii, Zh. Eksp. Teor. Fiz. **94**, 343 (1988) [JETP **67**, 625 (1988)].
[40] D. Braun and G. Montambaux, Phys. Rev. B **52**, 13903 (1995).
[41] C. L. Bertrand and A. M. García-García, Phys. Rev. B **94**, 144201 (2016).
[42] L. Benet, T. Rupp, and H. A. Weidenmüller, Phys. Rev. Lett. **87**, 010601 (2001).
[43] M. Srednicki, Phys. Rev. E **66**, 046138 (2002).
[44] C. E. Porter, *Statistical Theory of Spectra: Fluctuations* (Academic, New York, 1965).
[45] M. Kieburg, J. J. M. Verbaarschot, and S. Zafeiropoulos, Phys. Rev. D **92**, 045026 (2015).
[46] J. Maldacena, D. Stanford, and Z. Yang, arXiv:1606.01857.
[47] J. S. Cotler, G. Gur-Ari, M. Hanada, J. Polchinski, P. Saad, S. H. Shenker, D. Stanford, A. Streicher, and M. Tezuka, arXiv:1611.04650.